Analysis of Different Particle Decays via Simulation of GEANT3 & Data from ATLAS

Oren Kereth, Alon Shaaltiel and Gadi Ninio

November 29, 2021

Abstract

In this experiment, using the GEANT3 simulation[1], the invariant mass of π^0 and K_s^0 and the lifetime of K_s^0 were measured through the tracks, energies and momenta of their decay products. The measurements yielded $\frac{\left|M_0^{\pi^0}-M_{theory}^{\pi^0}\right|}{/M_{theory}^{\pi^0}}=1.9\%$ and $N\sigma=3.7$ for the invariant mass of π^0; $\frac{\left|M_0^{K_S^0}-M_{theory}^{K_S^0}\right|}{M_{theory}^{K_S^0}}=11\%$ and $N\sigma=3.7$ for the invariant mass of K_s^0 and $\frac{\left|\tau^{K_S^0}-\tau_{theory}^{K_S^0}\right|}{\tau_{theory}^{K_S^0}}=66\%$ and $N\sigma=8.3$ for the mean lifetime of K_s^0. Afterwards, using raw data from ATLAS, the mesons J/ψ , $\Upsilon(1S)$ and the boson Z^0 were identified via the pairing of electrons and positrons from about 900,000 events. The masses of J/ψ and $\Upsilon(1S)$ were then found through data driven background estimation and compared to the literature, yielding $N\sigma=2.4$ and $\frac{\left|M_0^{\Upsilon(1S)}-M_{0_{theory}}^{\Upsilon(1S)}\right|}{M_{0_{theory}}^{\Upsilon(1S)}}=1.8\%$ for $\Upsilon(1S)$ and $N\sigma=0.18$ and $\frac{\left|M_0^{J/\psi}-M_{0_{theory}}^{J/\psi}\right|}{M_{0_{theory}}^{J/\psi}}=0.45\%$ for J/ψ.

1 Theory

1.1 Fermions And Bosons

Particles are of two types: bosons and fermions. Fermions are particles with half-integral spin (1/2, 3/2...) who obey the Fermi-Dirac statistic while bosons are particles with integral spin (1,2...) who obey the Bose-Einstein statistic.

1.2 Antiparticles

Antiparticles were predicted by Dirac in 1931 [3]. Antiparticles have the same mass and lifetime as their corresponding particles but with opposite charge and magnetic moment. Their existence is a property of both fermions and bosons.

1.3 The Standard Model

1.3.1 The Fundamental Particles

According to the Standard Model all matter is built from fundamental spin $\frac{1}{2}$ fermions - quarks and leptons[3].

Leptons

There are 6 'flavours' of leptons. Three of them are charged with the exact same charge as the electron- electron (e), muon (μ) and tau(τ) ordered by mass from left to right such that tau is the heaviest of the trio and the electron is the lightest. The other three leptons are neutral and are paired with each flavour of charged lepton[3]. These are the neutrinos and their corresponding pair is denoted by their subscript- ν_e, ν_μ, ν_τalso with increasing mass from left to right.

Quarks

In resemblance to leptons, there are also 6 'flavours' of quarks. Unlike the fermions, quarks carry fractional charges of $\frac{2}{3}|e|$ or $-\frac{1}{3}|e|$.Quarks are grouped into pairs with increasing mass where each pair contains one positively charged particle and a negatively charged one (see Table 1).

Charge\Pair	1	2	3
$2/3\,\|e\|$	u (up)	c (charmed)	t (top)
$-1/3\,\|e\|$	d (down)	s (strange)	b (bottom)

Table 1: Pairing of the Quarks and their corresponding charges ordered by mass

While leptons exist as free particles, the same isn't true for quarks. Because of the strong interaction existing between quarks , quarks are only found in combinations referred to as 'Hadrons'. Two types of hadrons have been established in nature: baryons and mesons [3]. Baryons consist of three quarks (e.g the proton is the baryon uud) while mesons consist of one quark and one antiquark (e.g the neutral pion $\pi^0$is a meson consisting of u and anti-u or d and anti-d). It is necessary to introduce another degree of freedom for quarks- colorcharge. Unlike the electrical charge, which corresponds to the electromagnetic

interaction, color chrage corresponds to the strong interaction . A quark's color can take one of three values: red, green and blue while an antiquark (the anti particle of the quark) can take one of three 'anticolors': antired, antigreen and antiblue [3] .

1.4 The Interactions

There are four types of fundamental interactions, each described by the exchange of characteristic bosons [3](see Table 2)

The Interaction	The Mediator	Timescale of decay via the interaction
strong	gluon, G	$10^{-23}s$
electromagnetic	photon, γ	$10^{-20}s$
weak	$W^{\pm}, Z^0$	$10^{-10}s$
gravity	graviton, g	———

Table 2: The Fundamental Interactions and their corresponding boson mediators

As mentioned before, strong interactions are those responsible for the binding of quarks together, leading to the creation of mesons and baryons. They are mediated by the massless gluon. Electromagnetic interactions, which are mediated by the exchange of photons are responsible for many intermolecular phenomena. Weak interactions are slow processes (considering the strong and EM interactions) such as β-decay, and are mediated by $W^{\pm}, Z^0$. These bosons have masses of order 100 times the proton mass [3]. Gravitational interaction is the weakest amongst them yet every fundamental particle is interacting through it. It is supposedly mediated by the graviton. Charged leptons interact through the EM interaction, and the weak interaction while neutrinos interact weakly only. The quarks interact strongly, weakly and through the EM interaction.

1.5 Special Relativity

1.5.1 4-Momentum

Considering the high velocities of particles in the accelerator , special relativity must be applied when addressing the subject of decays and interactions. The 4-momentum of a particle is defined as

$$P^{\mu} = (E, \overrightarrow{p}) \tag{1}$$

where E is the particle's energy and $\overrightarrow{p}$ is its spacial momentum. The invariant mass of the particle, which is the same in all frames of reference can also be defined

$$M_0^2 = E^2 - \|\overrightarrow{p}\|^2 \tag{2}$$

where M_0 is the rest mass of the particle, the invariant mass. Using the invariant mass through this equality is a strong tool when addressing decays, as demonstrated below. In conjunction with the invariant mass, another fundamental conservation is that of the 4-momentum in a certain frame of reference, which along with the invariant mass can yield info about the particle (e.g its mass and energy). Suppose a particle decays into two particles whose momenta and masses are known $m_1, \overrightarrow{p}_1, m_2, \overrightarrow{p}_2$ where $m_1, \overrightarrow{p}_1$ are the corresponding mass and momentum of the first particle and $m_2, \overrightarrow{p}_2$are the corresponding mass and momentum of the second particle. Using the conservation of 4-momentum before and after the decay and the invariant mass in (2), one can derive the following relation

$$M_0^2 = m_1^2 + m_2^2 + 2\sqrt{m_1^2 + \|\overrightarrow{p_1}\|^2}\sqrt{m_2^2 + \|\overrightarrow{p_2}\|^2} - 2\,\|\overrightarrow{p}_1\|\,\|\overrightarrow{p}_2\|\,cos(\theta) \tag{3}$$

where θ denotes the angle between the two momenta. This equation will be of significant use during this experiment.

1.6 Charged Particle in a Magnetic Field

As explained in the following section, the particles will go through a spectrometer whose purpose is to measure the momentum of the particle. This is done by inducing a uniform magnetic field in a direction perpendicular to the direction of the particle's propagation for a known length, thus applying Lorentz force on the particle given by

$$F = qv_{\perp}B \tag{4}$$

where q is the particle's charge and $v_{\perp}$is the velocity in the direction perpendicular to the magnetic field. As a result of the force, the particle will deviate from its original track until it reaches the end of the spectrometer. The curvature of its trajectory can then be measured, (supposing it has an electric charge, otherwise this method will prove ineffective) and by using Newton's second law and the circular motion of the charged particle inside the spectrometer, the particle's momentum can be extracted using the equation

$$p_T = \frac{qB}{\kappa} \tag{5}$$

where p_T is the particle's momentum in the direction perpendicular to the magnetic field, its transverse momentum, and κ is the curvature of its trajectory inside the spectrometer. Using this method, the momentum of the decay products of different particles considering these products are charged can now be measured.

1.7 Decays

Let us look at a particle decay with a mean lifetime of τ. As τ can be extremely short in strong interactions, it is useful to define Γ, energy width through the uncertainty principle such that

$$\Gamma = \frac{\hbar}{\tau}$$

Γ represents the energy spread of the decaying particle. One can then measure the mass of the decaying particle using its decay products energies, the mass distribution (considering that the particles are relativistic) is given by

$$f_1(M; \Gamma, M_0) = \frac{a}{(M^2 - M_0^2)^2 + M_0^2\Gamma^2} \tag{6}$$

where a is a normalization factor, M_0 is the rest mass and also the resonance mass of the distribution, where the peak occurs. Instead of looking the at the mass (which is also energy) distribution, using the uncertainty principle as used before and a

Fourier transform to replace decay energies with decay times, one can get the lifetime distribution in the event of a particle decay

$$f_2(\tau;\tau_0) = be^{-\frac{\tau}{\tau_0}} \tag{7}$$

where b is a normalization factor and $\tau_0$is the mean lifetime which will be measured in this experiment.

1.8 Lifetime

Suppose a particle of rest mass M_0 and momentum p passes a distance L before decaying. Its lifetime τ in its rest frame is thus given by

$$\tau = \frac{M_0 L}{p} \tag{8}$$

1.9 Electromagnetic Interactions In Medium

In this experiment the energy of electromagnetic interacting decay products such as photons and electrons will be measured using an electromagnetic calorimeter (also called E-Cal). The photons and electrons passing through the E-Cal deposit their energy in it in several ways.

1.9.1 Photons' Energy Deposit

1)**The Photoelectric Effect:** A photon can deposit its entire energy by ionizing an electron from an atom and providing it with kinetic energy. Energy conservation must be maintained and therefore

$$E_\gamma = h\nu = I_B + T_e \tag{9}$$

where E_γ is the photons energy, ν is its frequency, I_B is the energy required to free the electron from the atom and T_e is the kinetic energy of the now free electron[2].

2) **Compton Scattering:** One can think of this process as the collision of a photon with frequency ν with a free electron at rest, thus delivering some of its energy and momentum to the electron. Unlike the photoelectric effect, the photon does not deposit its entire energy. The energy deposited by the photon into the medium in this case can be derived using 4-momentum conservation and mass invariance.

3) **Pair Production:** When a photon has sufficient energy, it can be absorbed into the medium and produce an electron-positron (the antiparticle of the electron) pair. This conversion can only occur by having the photon deliver some of its momentum , but very little energy to nearby nucleus, otherwise momentum-energy conservation is violated [2].

1.9.2 Electrons' Energy Deposit

1) **Ionization:** Electrons can ionize atoms in their path by interacting electromagnetically with the bound electrons, thus delivering some of their energy to the now free electrons.

2) **Bremsstrahlung:** When electrons accelerate or decelerate as a result of electromagnetic interactions with the medium, they emit energy in the form of photons. This form of energy loss becomes dominant in higher energies [2].

When a highly energetic photon or electron passes through the medium, it can create 'showers', these are avalanches of photons and electrons created by the original particle. Suppose that the original particle is a photon, it can therefore ionize atoms via the photoelectric effect. The resulting free electrons can now ionize atoms themselves or emit photons via bremsstrahlung and thus a 'shower' is created, ending with the deposit of all the energy of the energetic particle in the medium.

2 The Simulation and Calibration

2.1 The Simulation

The simulation consists of a magnetic spectrometer, EM calorimeter, iron yoke and muon chamber [1]. Each event starts with the generation and injection of a neutral or charged particle from a given list with a known energy. For particles traversing sensitive areas, the program stores 'hits'. At the end of the event processing, the program uses the hits to simulate the data produced by the detector, which includes raw data and also reconstructed parameters [1]. Suppose a e^- is injected into the detector with a momentum of $10\,GeV$, see Appendix A for the output.

2.1.1 The Magnetic Spectrometer

The Magnetic Spectrometer consists of 10 drift chambers inside a uniform magnetic field. The magnetic field applies a Lorentz force on charged particles, making them deviate from their original track as explained in 1.6. A chamber's dimensions are $3 \times 62 \times 60\,cm^3$ and the distance between two chambers is $8\,cm$. It consists of two planes of 5 anode and 6 cathode wires made of tungsten. The wires are strung parallel to the z-axis on a frame made of G10 material[1]. A measurement of the drift time on the sense wires allows measurement of the y position, needed for curvature determination. The measured hit positions are displayed in the graphical output as crosses [1]. When a charged particle passes through the spectrometer the simulation outputs its curvature, 'AKAPPA' , as seen in Appendix A and "TANDIP", the tangent of the dip angle which will be denoted as θ_{dip}.

2.1.2 The Electromagnetic Calorimeter (E-Cal)

The E-Cal's function is to detect and measure the energy and location of electrons, positrons and photons, which deposit their energy inside of it as explained in section 1.9 through showers of electrons, positrons and photons. It is simulated as an array of 650 BGO crystals positioned $10cm$ behind the magnetic spectrometer. The 'shower' then interacts with activators doped into the crystal that can be excited by electron-hole pairs produced by charged particles in the crystal lattice; these dopants can then de-excite through photon emission. These photons go through a

PMT (photo multiplier) which amplifies the signal linearly and outputs a pulse. The E-Cal measures the pulse-height, which is proportional to the energy deposited in each crystal [2]. The hits are represented on a front view of the detector as circles with the size of each circle proportional to the signal height in the corresponding crystal. The program attempts to associate the hit crystals into clusters and outputs the clusters locations and pulse heights[1].

2.1.3 Iron Yoke and Muon Chambers

The Iron Yoke is a hadron calorimeter (h-cal) designed to stop the hadrons by hadronic interactions. It is placed 10 cm behind the E-Cal. Two drift chambers similar to those of the magnetic spectrometer serve as a muon detector, which measures the position of charged particles that pass through it [1].

2.2 Calibration

In order to measure the momentum and energy of a particle moving through the detector, it is essential to calibrate the system. The strength of the induced magnetic field in the spectrometer must be known in order to extract the momentum of the particle from (5) given the curvature outputted by the simulation. The same applies for the conversion from pulse height outputted by the simulation as a result of a particle passing through the E-Cal to its energy. Therefore, particles with known mass and momentum were injected into the detector, their curvature and pulse heights were outputted and with these measurements one can find the magnetic field operating in the spectrometer, which will be symbolized by B_0 and the relationship between the pulse height and energy. More specifically, in order to measure B_0 electrons and muons (carrying a negative elementary charge) were injected at various momenta. Using (5) one can find the induced magnetic field using the transverse momentum and curvature. By injecting charged particles at various momenta one can plot a linear fit between the curvature and the inverse of the transverse momentum. The slope of the fit will be proportional to B_0 and other known constants. 10 momentum values were chosen starting at $10\,GeV$ all the way up to $100\,GeV$ with increments of $10\,GeV$ between them. 10 injections were made for each value. The averages of κ and P_T^{-1} were taken as the representing measurement for each momentum. The same number of photons, with the same momenta were injected as well. The average of the pulse height for each momentum value was taken as the representing measurement. Using the measurements of curvature collected from the muons and electrons (but not from the photons as they are electrically neutral) and the measurements of pulse height collected from the electrons and photons (but not from the muons, as they do not deposit their entire energy in the E-Cal), the magnetic field and the relationship between pulse height and energy can be characterized.

2.2.1 Extracting The Magnetic Field

Suppose a particle with momentum p and charge e is injected into the detector, given θ_{dip} which can be calculated using arctan on 'TANDIP' , the momentum perpendicular to the magnetic field can be calculated

$$p_T = pcos(\theta_{dip}) \tag{10}$$

From (5) using the measurements of the electrons and muons and (10), a fit of the form

$$\kappa = \frac{a_0}{p_T} + a_1 \tag{11}$$

was done. Where a_0 according to (5) with slight modifications due to the simulation is $a_0 = \frac{|e|B_0}{2}$ and $a_1$is expected to be 0 or near that value. Two fits of the form in (11) were made, one for the electrons and the other for muons. The average of $a_0$was then calculated, from which the magnetic field B_0 was extracted.

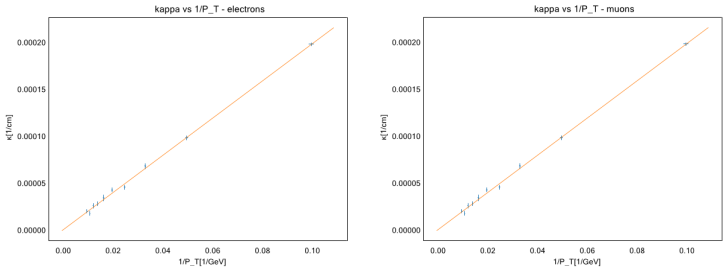

(a) Electrons fit (b) Muons fit

Figure 1: Linear fits of the measured curvature of the trajectory, κ (measured in $\frac{1}{cm}$) as a function of one over the electrons/muons transverse momentum, $\frac{1}{p_T}$(measured in $\frac{1}{GeV}$) calculated using the particle's momentum through (10)

The fit parameters for each of the fits are given by (see Table 3)

Electrons	
$a_0 \pm \Delta a_0$ GeV/cm(Relative Error)	$a_1 \pm \Delta a_1$ 1/cm(Relative Error)
$2.000E-03 \pm 3.1E-05(1.6\%)$	$-8.0E-07 \pm 1.15E-06(140\%)$
Muons	
$a_0 \pm \Delta a_0$ GeV/cm(Relative Error)	$a_1 \pm \Delta a_1$ 1/cm(Relative Error)
$2.000E-03 \pm 3.1E-05(1.6\%)$	$4.6E-07 \pm 1.00E-06(220\%)$

Table 3: Fit parameters and statistics of the linear fits of the curvature of the trajectory, κ as a function of one over the transverse momentum, $\frac{1}{p_T}$

and the average fit parameters are as follows (see Table 4)

Parameter	Value	Error(Relative Error)
a_0^{AVG} GeV/cm	$2.000E-03$	$2.2E-05(1.1\%)$
a_1^{AVG} 1/cm	$-1.7E-07$	$7.6E-07(440\%)$

Table 4: Average fit parameters of the linear fits of the curvature of the trajectory, κ as a function of one over the transverse momentum, $\frac{1}{p_T}$

The magnetic field was extracted and is given by $B_0 = 1.334403 \pm 2.9 \cdot 10^{-5} T$ with a relative error of 0.0022%. $a_1$is consistent with the expected value of 0.

In both fits the statistics (see Appendix B) and the plots indicate a very high correlation with the theory.

2.2.2 Pulse Height

To correlate between pulse height and the energy of the particle traversing through the E-Cal, two linear fits were made. One fit was of the electrons and the other of the photons injected into the detector. The fits made were of the form

$$P = b_1 P.H + b_2$$

where P is the momentum of the particle sent (which is its energy for photons and approximately its energy for electrons considering its mass is negligible compared to it) and $P.H$ is the total pulse height outputted by the simulation associated with that particle.

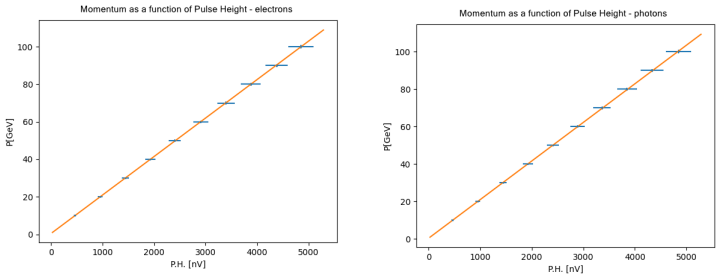

(a) Electrons fit (b) Photons fit

Figure 2: Linear fits of the electrons'/photons' momentum P (measured in GeV) as a function of the measured pulse height of the particle (measured in nV)

The fit parameters for each of the fits are given by (see Table 5)

Electrons	
$b_1 \pm \Delta b_1$ GeV/nV(Relative Error)	$b_2 \pm \Delta b_2 GeV$(Relative Error)
$2.0508E-02 \pm 2.4E-05(0.12\%)$	$4.95E-01 \pm 2.9E-02(5.9\%)$
Photons	
$b_1 \pm \Delta b_1$ GeV/nV(Relative Error)	$b_2 \pm \Delta b_2 GeV$(Relative Error)
$2.0621E-02 \pm 2.9E-05(0.14\%)$	$4.07E-01 \pm 3.5E-02(8.6\%)$

Table 5: Fit parameters and statistics of the linear fits of the curvature of the trajectory, κ as a function of one over the transverse momentum, $\frac{1}{p_T}$

and the average fit parameters are as follows (see Table 6)

Parameter	Value	Error(Relative Error)
b_1^{AVG} GeV/nV	$2.0600E-02$	$1.9E-05(0.092\%)$
$b_2^{AVG} GeV$	$4.51E-01$	$2.3E-02(5.0\%)$

Table 6: Average Fit Parameters of the linear fits of the curvature of the trajectory, κ as a function of one over the transverse momentum, $\frac{1}{p_T}$

In both fits the statistics (see Appendix B) and the plots indicate a good fit and an overestimation of the error term on the pulse-height.

3 Measurements and Results

In this part of the experiment, the particles π^0 and K_s^0 were injected into the detector. Their decays were analysed and through the decay products their invariant mass was calculated and their mean lifetime (calculated only for K_s^0 for reasons detailed later). The magnetic field in the spectrometer can be adjusted via a parameter α in the simulation which factors the magnetic field. $\alpha = 1$ for the measurements of π^0 and was changed to $\alpha = 4$ for the measurements of K_s^0.

3.1 Measurements Concerning π^0

The meson π^0 is made up of an $u\ \overline{u}$ pair or $d\ \overline{d}$ pair. Its invariant mass is $M^{\pi^0}_{PDG} = 1.3497680 \times 10^{-1} \pm 5.0 \times 10^{-7} GeV$ [4] and its mean lifetime is $\tau_{\pi^0} = (8.43 \pm 0.13) \times 10^{-17} s$. In the vast majority of cases (99%) π^0 decays into two photons 2γ. Decays occurring via this decay mode have two distinct clusters (one for each photon) in the E-Cal and have no tracks in the spectrometer (since they have no electric charge, this also implies they move in straight lines through it) will be considered "interesting events" and will be the subject of measurements in this part. However, if an event contains tracks or more than 2 clusters it will not be counted as it is a bug in the simulation, and if there are less than 2 clusters the method of extracting the invariant mass will not work. Other decay modes will be counted but will not be analyzed. And so, these measurements will be discarded. The branching ratio of the interesting decay mode will be compared with the expected value of 99%. Because of its short mean lifetime compared with the resolution of the detector, π^0's lifetime will not be measured in this experiment and only its invariant mass will be plotted. In addition to that, it is assumed that π^0decays right at the injection point.

3.1.1 Invariant Mass of π^0

The invariant mass of π^0 will be measured using (3). Since photons have no mass their energies and momenta are the same and their invariant mass is 0. Using the calibration and pulse heights, the energies of the photons will be measured. Using the location of the clusters for each of the photons and under the assumption that π^0decays instantly upon injection, the cosine of the

angle between the momenta of the photons was calculated via the relation

$$cos(\theta) = \frac{\overrightarrow{r}_1 \cdot \overrightarrow{r}_2}{\|\overrightarrow{r}_1\| \, \|\overrightarrow{r}_2\|} \tag{12}$$

where $\overrightarrow{r}_1, \overrightarrow{r}_2$ are the two position vectors for each of the clusters after adding $10\,cm$ to the x component because the particles are injected at $x = -10\,cm$.

3.1.2 Mass Distribution of π^0

586 π^0 were injected into the detector with a momentum of $5\,GeV$ (according to the simulation). Out of the 586 events, 13% were discarded due to bugs and the remaining 87% (509 events) were all characterized by no track and 2 clusters in the E-Cal, resulting in a branching ratio of 100% for the decay $\pi^0 \to 2\gamma$ in "interesting events". From every interesting event, the invariant mass of π^0 was calculated using (3) and (3). Afterwards, a histogram with 80 bins, each with width of $1.4 \cdot 10^{-3}\,GeV$ was made. The average mass in each bin was then taken as the representing measurement of that bin. The number of events in each bin should distribute according to (6). Therefore, a Breit-Wigner fit of the form

$$Events_{\pi^0}(M) = \frac{a_0}{(M^2 - a_1^2)^2 + a_1^2 a_2^2} \tag{13}$$

was made, where a_0 is the normalization factor and a_1, a_2 represent the invariant mass of π^0, $M_0^{\pi^0}$ and the energy width, Γ respectively.

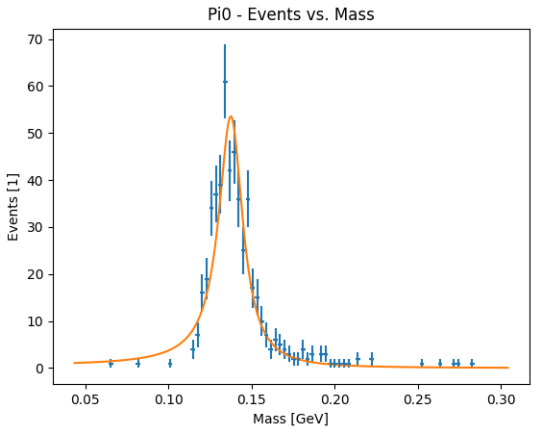

Figure 3: Breit-Wigner distribution fit for the mass histogram of π^0

The fit parameter are as follows (see Table 7)

π^0		
Parameter\Statistic	Value	Error(Relative Error)
a_0 $^{\text{Events}}/_{\text{GeV}^2}$	$3.18 \cdot 10^{-4}$	$3.5 \cdot 10^{-5}(11\%)$
$a_1\,GeV$	$1.3761 \cdot 10^{-1}$	$7.1 \cdot 10^{-4}(0.51\%)$
$a_2\,GeV$	$1.77 \cdot 10^{-2}$	$1.5 \cdot 10^{-3}(8.4\%)$
χ^2_{red}	1.1	—
P_{value}	0.24	—

Table 7: Fit parameters and statistics of the BW distribution fit for the mass histogram of π^0

Using the fit parameters and (13) the invariant mass of π^0 was extracted

$$M_0^{\pi^0} = 1.3761 \cdot 10^{-1} \pm 7.1 \cdot 10^{-4}\,GeV\,(0.51\%\,error)$$

The extracted value was then compared with the one taken from the literature [4] resulting in: $N\sigma = 3.7$ and $\frac{\left|M_0^{\pi^0} - M_{theory}^{\pi^0}\right|}{M_{theory}^{\pi^0}} = 1.9\%$.
These statistics and metrics indicate a good fit and correlation with the theory.

3.1.3 Discussion

The results are in clear agreement with the theory and are statistically significant. This is accompanied by the simulation's $\pi^0 \to 2\gamma$ branching ratio, 100%, which is very close to the theoretical value, 99% [4]. However, there is still a problem which has not been addressed.
There is a discrepancy between the fit line and number of events at the lower range of the mass spectrum. A possible cause for this discrepancy is the method of measurement, specifically how the angle between the photons is measured. The method requires 2 distinct pulse-height clusters, which means the sum of the showers' widths must be smaller than the distance between them. For a sufficiently energetic particle or a small enough angle, 2 clusters are impossible. This, in turn, means that below a certain angle measurements are much more likely to be discarded. Noting the fact that the invariant mass squared is proportional to $1 - \cos\theta$, it is clear why the measurements are lacking in events with a small invariant mass. If said events were not missing, the fit would have shifted left such that the extracted invariant mass will decrease and get closer to the theoretical value.

3.2 Measurements concerning K_S^0

The meson K_S^0 is made up of a $d\,\bar{s}$ pair. Its invariant mass is $M_{theory}^{K_S^0} = 4.97611 \cdot 10^{-1} \pm 1.3 \cdot 10^{-5}\,GeV$ [4] and its mean lifetime is $\tau_{K_S^0} = 8.9564 \cdot 10^{-11} \pm 3.3 \cdot 10^{-14}\,s$. The lifetime, $c\tau_{K_S^0} = 2.6844\,cm$ is of the same order as the spectrometer's resolution, meaning the particle decays along the path from the injection point to the E-Cal. K_S^0's two most common decay modes, which together occur 99.9% of the time, are $K_S^0 \to \pi^0\pi^0$ (30.7%) and $K_S^0 \to \pi^+\pi^-$ (69.2%) [4]. This experiment will not consider

any other decay modes. As was mentioned in the previous section, π^0 decays instantaneously (when compared with the resolution of the spectrometer) via $\pi^0 \to 2\gamma$. Photons or π^0 particles leave no trace in the spectrometer which makes locating the vertex of the decay impossible. The vertex of the decay is necessary in the calculation of the lifetime, which should be measurable using the $K_S^0 \to \pi^+\pi^-$ decay mode. $\pi^\pm$ have an elementary charge corresponding to their sign and a lifetime of $c\tau_{\pi^\pm} = 7.8045\,m$ [4] which is significantly greater than the length of the measurement apparatus, and so, it is assumed they do not decay. As $\pi^\pm$ are hadrons they do not deposit their entire energy inside the E-Cal and their momentum must be measured in some other way. The $\pi^\pm$ particles are charged and therefore have their trajectories curved by the magnetic field and leave a trace in the spectrometer. Using (5) and the curvature outputted by the simulation, it is possible to measure the transverse momentum of each particle. Using conservation of 3-momentum, the angle between the particles at the decay vertex, and the position of the vertex (see Appendix E), it is possible to calculate both the invariant mass and the lifetime of K_S^0. It is clear then that this is the decay mode of interest. As with the previous section, some events make measurement impossible or incorrect, if produced by a bug in the simulation, thus, an "interesting event" must be defined, all other events (excluding those which did not register in any detector) will be counted and promptly discarded. An "interesting event" will have 2-3 tracks (which are identified by the simulation), opposite curvatures in the chosen tracks (if there are 3) and the tracks must share a vertex. In case there are 3 tracks, the two tracks with the most hits are taken. In order to compare the branching ratio of the different decay modes to the theoretical value each event is classified into $K_S^0 \to \pi^0\pi^0$, $K_S^0 \to \pi^+\pi^-$ or BUG. A BUG is an event with more than 5 pulse-height clusters or with no interaction with the E-Cal and spectrometer. These events are discarded without being considered in the branching ratio, they account for 3.8% of the events. As it is simpler to define what a $K_S^0 \to \pi^0\pi^0$ event registers, it is assumed that all events which are not a BUG or a $K_S^0 \to \pi^0\pi^0$ are $K_S^0 \to \pi^+\pi^-$ events. And so, a $K_S^0 \to \pi^0\pi^0$ event is expected to have a pulse-height cluster(s) and no track. In the simulation, $K_S^0 \to \pi^0\pi^0$ account for 44% of events, thus, $K_S^0 \to \pi^+\pi^-$ account for 56% of events.

3.2.1 Invariant Mass of K_S^0

The invariant mass of K_S^0 will be measured using (3). The mass of $\pi^\pm$ is $M_{theory}^{\pi^\pm} = 1.395704 \cdot 10^{-1} \pm 1 \cdot 10^{-7}\,GeV$ [4], and their momenta will be calculated using (5) and the calibration, the angle between the particles is given by the simulation as "Phi" at the vertex.

3.2.2 Mass Distribution of K_S^0

2015 K_S^0 were injected into the detector with a momentum of $10\,GeV$ (according to the simulation). Out of the 2015 events, 14% (286 events) were "interesting events" used to calculate the invariant mass of K_S^0 was calculated using (3). Afterwards, a histogram with 7 bins, each with width of $2.9 \cdot 10^{-2}\,GeV$ was made. The average mass in each bin was then taken as the representing measurement of that bin. Just as with π^0, the invariant mass should distribute according to (6), and so, a fit of the form presented in (13) was made.

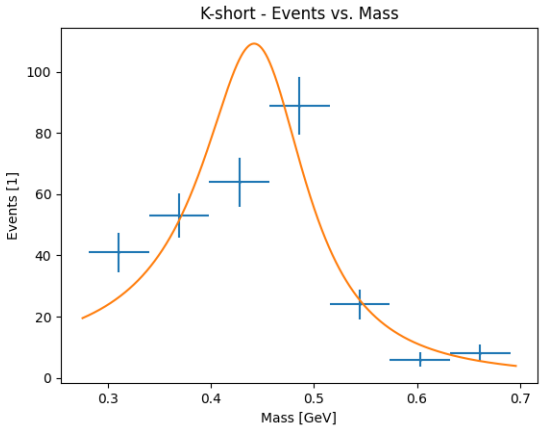

Figure 4: Breit-Wigner distribution fit for the mass histogram of K_S^0

The fit parameter are as follows (see Table 8)

K_S^0 Invariant Mass		
Parameter\Statistic	Value	Error(Relative Error)
$a_0[^{\text{Events}}/_{\text{GeV}^2}]$	$3.39 \cdot 10^{-1}$	$1.3 \cdot 10^{-2}(38\%)$
$a_1[GeV]$	$4.42 \cdot 10^{-1}$	$1.5 \cdot 10^{-2}(3.5\%)$
$a_2[GeV]$	$1.26 \cdot 10^{-1}$	$5.1 \cdot 10^{-2}(40\%)$
χ^2_{red}	1.4	—
P_{value}	0.22	—

Table 8: Fit parameters and statistics of the BW distribution fit for the mass histogram of K_S^0

Using the fit parameters and (13) the invariant mass of K_S^0 was extracted

$$M_0^{K_S^0} = 4.42 \cdot 10^{-1} \pm 1.5 \cdot 10^{-2}\,GeV\,(3.5\%\,error)$$

The extracted value was then compared with the one taken from the literature [4] resulting in: $N\sigma = 3.7$ and $\frac{\left|M_0^{K_S^0} - M_{theory}^{K_S^0}\right|}{M_{theory}^{K_S^0}} = 11\%$.
The statistics show a good correlation with the theory, yet the fit itself does not have a definite peak correlating to the data, as the peak in the data is more to the right. The metrics show that the measured values are far from the theoretical values compared to their error and value.

3.2.3 Lifetime of K_S^0

The lifetime of K_S^0 will be calculated using (8). Each event has a measured invariant mass which will be used. The length L is

calculated using the vertex's position after adding $10\,cm$ to the x axis, since the injection point is at $x = -10\,cm$. The momentum's, p, calculation is in Appendix E. A histogram with 45 bins, each with a width of $1.1 \cdot 10^{-11}\,s$ was made. The average lifetime in each bin was then taken as the representing measurement of that bin. The number of events in each bin should distribute according to (7). Therefore, an exponential fit of the form

$$Events_{K_S^0}(\tau) = a_0 e^{-\frac{\tau}{\tau_0}} + a_1 \tag{14}$$

was made (see Figure 5). Where a_0 is the normalization factor, a_1 is a free parameter expected to be 0 and τ_0 is the mean lifetime of K_s^0 later compared with the theoretical value.

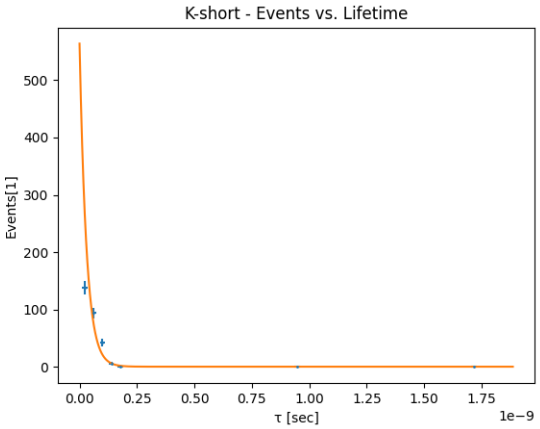

Figure 5: Exponential distribution fit for the lifetime histogram of K_S^0

The fit parameter are as follows (see Table 9)

K_s^0 Lifetime		
Parameter\Statistic	Value	Error(Relative Error)
$a_0[Events]$	560	360 (63%)
$\tau_0[s]$	$3.03 \cdot 10^{-11}$	$7.1 \cdot 10^{-12}$ (24%)
$a_1[Events]$	$5.7 \cdot 10^{-1}$	$9.5 \cdot 10^{-1}$ (170%)
χ^2_{red}	2.0	—
P_{value}	0.093	—

Table 9: Fit parameters and statistics of the exponential distribution fit for the lifetime histogram of K_S^0

The extracted value for τ_0 was compared with the one taken from the literature [4] resulting in: $N\sigma = 8.3$ and $\frac{\left|\tau^{K_S^0} - \tau^{K_S^0}_{theory}\right|}{\tau^{K_S^0}_{theory}} =$ 66% which indicate that the extracted value is far from the theoretical one, though the statistical parameters and graphs indicate a good fit was made.

3.2.4 Discussion

Both mass and lifetime's theoretical distributions have been statistically validated, and $K_S^0 \to \pi^+\pi^-$ is still the most common decay mode and occurs the majority of the time. However, the branching ratios are different from the theoretical values. In addition, both extracted values are far from their theoretical counterparts to differing degrees. K_S^0's invariant mass histogram plummets, when a smooth transition is expected. Possible causes for this drop are the filters and the simulation's track recognition and fit, in the following ways. There are 69 events with 2-3 tracks which may have a vertex between two tracks, however these vertices do not include the two tracks with the highest number of hits. Were all 69 included it would have a profound effect on the histogram. Another possible cause is if a track is counted twice. Suppose tracks 1 and 2 have more hits than track 3 but track 1 is alongside track 2 and is a result of a bug. Then the vertex of tracks 1 and 2 which the analysis looks for either doesn't exist and the event is thrown out, or the vertex exists and tracks 1 and 2 have the same sign of curvature thus event is thrown out. This likely accounts for many events with 3 tracks which were thrown out after both prevalent curvatures had the same sign. As these types of bugs are much more likely at higher energies the histogram is missing higher mass values. And as the lifetime is directly related to the invariant mass (See (8)) it is clear why a warped invariant mass distribution leads to a warped lifetime distribution. The lifetime is dependent on other measurements which may have also been adversely affected by the event filters and simulation. Regardless, both the lifetime and invariant mass share the same scale as their corresponding theoretical values.

4 ATLAS

4.1 The Data

The particle data which is analysed during this part has been provided by the ATLAS particle accelerator. The data details detected electrons and positrons, their position in the detector using the angles η and φ, the measured transverse momentum of each particle, and the confidence of the detector that the particle is a positron or an electron using 3 Boolean values, "Loose", "Medium" and "Tight". "Loose" represents that the detector is not very confident of the particle's type, "Medium" is more confident and "Tight" is the most confident. To get a meaningful measurement out of this limited data set some assumptions concerning the decays must be made. It is assumed that all electrons and positrons in the data set were formed in a $X^0 \to e^-e^+$ decay, where X^0 is the particle(s) to be identified. Were it known which electrons and positrons came from an X^0 decay, it may be possible to identify X^0 by its invariant mass, using a Breit-Wigner fit on a histogram similarly to (13). The identification is further simplified because of the assumed decay mode, which implies X^0 is not a lepton, is neutral and that such a decay mode exists. As it is unknown which particles, and specifically, pairs came from which decay, the invariant mass of X^0 is calculated for all possible e^-e^+ pairs in a particular event (i.e. if an event contains the measurements of 3 particles, e_1^-, e_2^-, e_3^+ the invariant masses $M_{1,3}^{X^0}$, and $M_{2,3}^{X^0}$ are calculated and associated with that

event) all calculated masses are added to the mass histogram. One expects an e^-e^+ pair which was not formed together will introduce noise into the mass histogram, this noise has no definite distribution function and is modeled at a later stage. On the other hand, an e^-e^+ pair which formed in a $X^0 \to e^-e^+$ decay will contribute a mass which distributes according to (6) with an invariant mass of M^{X^0}. Thus, a Breit-Wigner distribution with some background is expected. The "Loose" measurements are expected to have more noise than "Medium" and "Tight", as they may contain particles which decayed in a decay mode with no e^-s or e^+s, and thus, pairing the two only introduces noise. The same is expected when comparing "Medium" to "Tight".

4.2 Tight Electrons Histogram

Pairing only tight electrons, a histogram containing 900 bins was plotted, with energies ranging between $1\,GeV$ to $150\,GeV$.

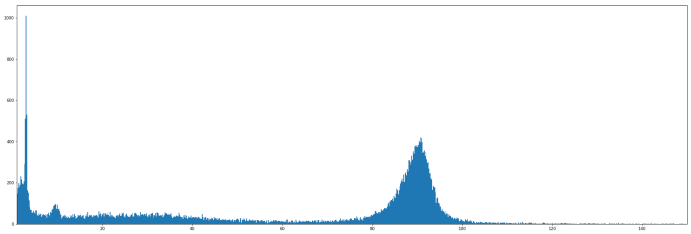

Figure 6: Tight electrons histogram. Contains 900 bins with energies ranging from $1GeV$ to $150GeV$.

Three peaks can be seen in the histogram: one at around $90GeV$, one at about $9.5GeV$ and one at about $3.1GeV$. Each of these peaks can be linked to a particle, where the rightmost resonance at around $90GeV$ corresponds the Z^0 boson, the resonance at around $9.5GeV$ corresponds to the $\Upsilon(1S)$ meson and the resonance at about $3.1GeV$ corresponds to the J/ψ meson.

4.3 Fit & Background Estimation

To extract the masses of the particles from the histogram a fit needs to be made and plotted. However, fitting the surroundings of the resonances according to the Breit-Wigner distribution to find a particle's mass would prove wrong, as there is irreducible background resulting from the pairing of one electron and one positron which are not decay products of the same particle. Therefore, a data driven background estimation was used. To estimate the background noise at the signal region (SR, where little background noise has been detected and mainly signal exists), far enough from the SR (where little signal has been detected and mainly background noise exists), two control regions (CR) which surround the SR and contain little signal and much noise were approximated. Using both CRs, a fit has been made for the background noise around each of the resonances. Using the fitted function, denoted by $BKG(M)$ where M is the invariant mass, a final fit over the SR and the CRs consisting of $BKG(M)$ and a signal function (Breit-Wigner distribution fit) whose parameters were fitted. From the fit parameters the rest mass of the particle was then extracted . According to these steps two fits were done, one for the resonance of the J/ψ meson and the other for the resonance of the $\Upsilon(1S)$ meson.

4.3.1 The J/ψ Meson

The region of measurement (CRs+SR) is from $1\,GeV$ to $7\,GeV$. The CR region to the left of the SR was bounded by $1\,GeV$ & $2.58\,GeV$ and the CR region to the right of the SR was bounded by $3.4\,GeV$ & $7\,GeV$. That data was then fitted to a normal distribution of the form

$$BKG^{J/\psi}(M) = A_0 e^{-(\frac{M-A_1}{A_2})^2} + A_3 \tag{15}$$

Afterwards, a fit containing the BKG function was made to the data in the region, extracted from a histogram in that region containing 30 bins. The fit is of the form

$$FIT^{J/\psi}(M) = BKG^{J/\psi}(M) + BW(M; a^{J/\psi}, \Gamma^{J/\psi}, M_0^{J/\psi}) \tag{16}$$

where BW is the Breit-Wigner distribution according to (6) and where the parameters in $BKG^{J/\psi}(M)$ are given from the previous fit. The fit parameters and plot are given by (see Table 10 and Figure 7, for the BKG function fit parameters see Appendix C)

Signal+BKG		
Parameter\Statistic	Value	Error(Relative Error)
$a^{J/\psi}[Events]$	230	130(57%)
$\Gamma^{J/\psi}[GeV]$	$1.53 \cdot 10^{-1}$	$4.1 \cdot 10^{-2}(27\%)$
$M_0^{J/\psi}[GeV]$	3.111	$7.9 \cdot 10^{-2}(2.5\%)$
χ^2_{red}	2.2	—
P_{value}	$2.9 \cdot 10^{-4}$	—

Table 10: Fit parameters of the signal+background fit in the range $[1GeV, 7GeV]$ for J/ψ

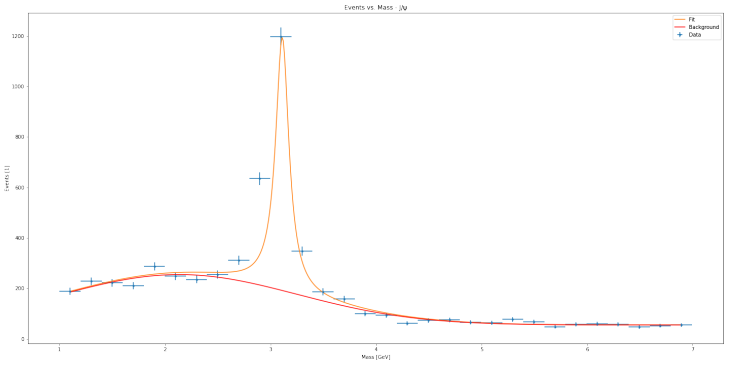

Figure 7: Plot of data(crosses), background fit ($BKG^{J/\psi}$, in red) and fit ($FIT^{J/\psi}$,in orange) in the range $[1GeV, 7GeV]$ for the particle J/ψ

Comparing the invariant mass extracted from the fit, $M_0^{J/\psi}$, to that taken from the literature $M_{0_{theory}}^{J/\psi} = 3.0969000 \pm 6.0 \cdot$

$10^{-6} GeV$ results in $N_\sigma = 0.18$ and $\frac{\left|M_0^{J/\psi} - M_{0_{theory}}^{J/\psi}\right|}{M_{0_{theory}}^{J/\psi}} = 0.45\%$ indicating a close relation between the two values.

4.3.2 The $\Upsilon(1S)$ Meson

The region of measurement (CRs+SR) is from $5\,GeV$ to $15\,GeV$. The CR to the left of the SR was bounded by $5GeV$ & $8.34GeV$ and the CR to the right of the SR was bounded by $11.02GeV$ & $15GeV$. The data from both CRs was then fitted to an exponent of the form

$$BKG^{\Upsilon(1S)}(M) = B_0 e^{B_1 M} + B_2 \tag{17}$$

Afterwards, a fit containing the BKG function was made to the data in the entire region of measurement, extracted from a histogram in that region containing 30 bins. The fit is of the form

$$FIT^{\Upsilon(1S)}(M) = BKG^{\Upsilon(1S)}(M) + BW(M; a^{\Upsilon(1S)}, \Gamma^{\Upsilon(1S)}, M_0^{\Upsilon(1S)}) \tag{18}$$

where BW is the Breit-Wigner distribution according to (6) and where the parameters in $BKG^{\Upsilon(1S)}(M)$ are given from the previous fit, just as for J/ψ. The fit parameters and plot are given by (see Table 11 and Figure 8, for the BKG fit parameters see Appendix D)

Signal+BKG		
Parameter\Statistic	Value	Error(Relative Error)
$a^{\Upsilon(1S)}[Events]$	8100	2600(32%)
$M_0^{\Upsilon(1S)}[GeV]$	9.628	$7.1 \cdot 10^{-2}(0.74\%)$
$\Gamma^{\Upsilon(1S)}[GeV]$	$6.0 \cdot 10^{-1}$	$3.3 \cdot 10^{-1}(55\%)$
χ^2_{red}	0.99	—
P_{value}	0.48	—

Table 11: Fit parameters of the signal+background fit in the range $[5GeV, 15GeV]$ for $\Upsilon(1S)$

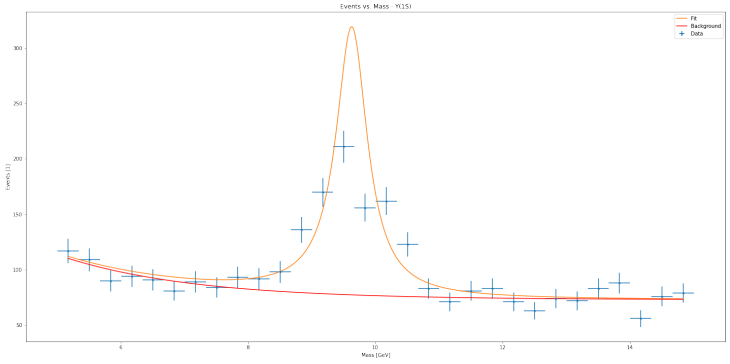

Figure 8: Plot of data (crosses), background fit ($BKG^{\Upsilon(1S)}$, in red) and fit ($FIT^{\Upsilon(1S)}$,in orange) in the range $[5GeV, 15GeV]$ for the particle $\Upsilon(1S)$

Comparing the invariant mass extracted from the fit, $M_0^{\Upsilon(1S)}$, to that taken from the literature $M_{0_{theory}}^{\Upsilon(1S)} = 9.46030 \pm 2.6 \cdot 10^{-4}\,GeV$ results in $N_\sigma = 2.4$ and $\frac{\left|M_0^{\Upsilon(1S)} - M_{0_{theory}}^{\Upsilon(1S)}\right|}{M_{0_{theory}}^{\Upsilon(1S)}} = 1.8\%$ indicating a close relation between the two values.

4.4 Discussion

Although the statistical values for the final fit of J/ψ are not ideal, it is evident the invariant mass is close to the theoretical one. Perhaps a change in the BKG function, or in the number of histogram bins would have improved the fit. Nevertheless, it remains true the fitted function describes both the signal and the background noise in all regions adequately. The same holds for $\Upsilon(1S)$, whose distribution statistically validated the theory. $\Upsilon(1S)$'s extracted invariant mass is close, both by value and by estimated error, to its theoretical counterpart. However, the extracted invariant mass has turned out a little bigger than it should have been. The peak of the fitted function (see Figure 8) comes out to the right of the histogram's peak, which in turn affects the invariant mass extracted from the fit. This may be resolved by a change to the histogram's resolution (bins) and continued guesswork of the initial parameters. Regardless, both fits came out well, yielding results comparable to those in the literature.

5 Conclusions

Starting with the simulation's calibration, the measured magnetic field is of the same order as those used at the LHC [5]. And the conversion between the measured aggregated pulse-height to particle energy was statistically validated. Following the calibration, π^0's invariant mass was extracted, resulting in $M_0^{\pi^0} = 1.3761 \cdot 10^{-1} \pm 7.1 \cdot 10^{-4}\,GeV$. As mentioned in the relevant discussion, the value is close to the theoretical one; however, $N\sigma$ is outside of the desired range. A possible explanation lies in the lack of lower mass events, which correlates with the inability to distinguish between 2 separate clusters at smaller scattering angles. To distinguish between closer clusters one should inject π^0 at lower momenta, improve the E-Cal's sensitivity, its spatial resolution and the simulation's ability to differentiate two overlapping clusters. K_S^0's invariant mass and lifetime were also extracted, resulting in $M_0^{K_S^0} = 4.42 \cdot 10^{-1} \pm 1.5 \cdot 10^{-2}\,GeV$ and $\tau^{K_S^0} = 3.03 \cdot 10^{-11} \pm 7.1 \cdot 10^{-12}\,s$. These values have the same scale as the theoretical ones, which are not close to those extracted in this experiment. This could be explained by the existence of bugs in the simulation, which lead to the disposal of events with higher invariant masses. Afterwards, using raw data from ATLAS, the mesons J/ψ,$\Upsilon(1S)$ and the boson Z^0 were identified through the pairing of electrons and positrons detected in each of the 900,000 events. By applying a data driven estimation in order to account for the irreducible background created as a result of wrong pairings of electrons and positrons, the invariant masses of J/ψ and $\Upsilon(1S)$ were extracted; $M_0^{\Upsilon(1S)} = 9.628 \pm 0.071\,GeV$ and $M_0^{J/\psi} = 3.111 \pm 0.079\,GeV$, both are close to their corresponding theoretical values. Overall, despite the staggering amount of bugs encountered throughout the experiment, satisfactory results has been achieved, proving the accuracy and effectiveness of the applied experimental methods and theoretical knowledge.

6 Appendix

Appendix A - GEANT3 Output From an e^- Injection At $10\,GeV$ and :

(a) Simulation instructions

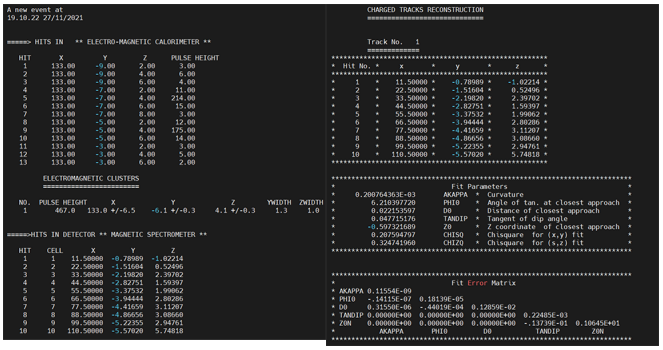

(b) Simulation output after a e^- injection at $10\,GeV$

Figure 9: GEANT3 Simulation instructions and output from a e^- injection at 10 GeV

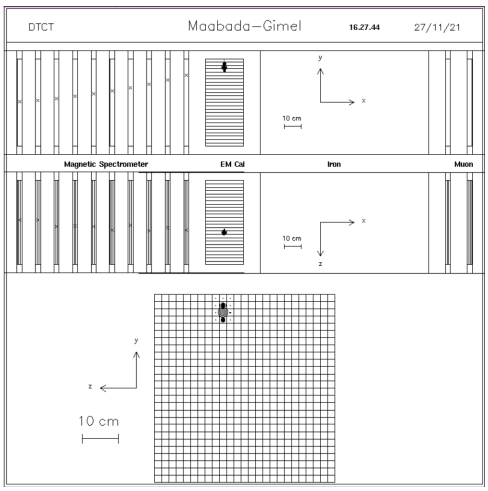

Figure 10: Example of an e^- injection event on the graphical display of the simulation. It consists of three projections: a side view on the x-y plane, a top view on the xz plane, and a front view of the EM calorimeter on the y-z plane. The particles are injected in the positive x direction, and the magnetic field is parallel to the z coordinate. The display includes the axis orientation, and scales for each projection. The crosses stand for the hits in the drift chambers (the magnetic spectrometer, or the muon chambers). The size of the circles in the EM calorimeter is proportional to the pulse height in the corresponding BGO crystal. [1]

Appendix B - Statistical Values of The Calibration Fits

Calibration	Fit	χ^2_{red}	P_{value}
Spectrometer Calibration	Electrons	1.0	0.40
	Muons	1.0	0.42
E-Cal Calibration	Electrons	$2.5E-03$	1.0
	Photons	$3.5E-03$	1.0

Table 12: Statistical values of the calibration fits

Appendix C - BKG Fit Parameters of J/ψ

BKG(J/ψ)	——	——	——
Parameter\Statistic	Value	Error	Relative Error
$A_0[Events]$	199.8	9.7	4.9%
$A_1[GeV]$	2.135	0.090	4.2%
$A_2[GeV]$	1.58	0.11	6.9%
$A_3[Events]$	54.8	3.3	6.0%
χ^2_{red}	1.6	——	——
P_{value}	0.032	——	——

Table 13: Fit parameters of the background fit in CR for J/ψ

Appendix D - BKG Fit Parameters of $\Upsilon(1S)$

BKG($\Upsilon(1S)$)	——	——	——
Parameter\Statistic	Value	Error	Relative Error
$B_0[Events]$	450	560	120%
$B_1[1/\text{GeV}]$	-0.48	0.22	46%
$B_2[Events]$	73.0	3.3	4.5%
χ^2_{red}	0.95	——	——
P_{value}	0.52	——	——

Table 14: Fit parameters of the background fit in CR for $\Upsilon(1S)$

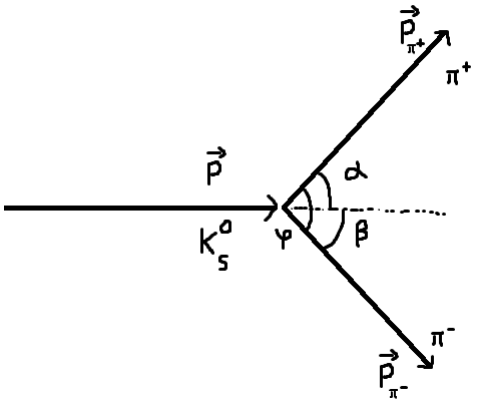

Figure 11: K^0_S decay into $\pi^+\pi^-$

Appendix E - Calculation of K^0_S's Momentum

The momentum p of K^0_S will be calculated using momentum conservation in the lab's frame of reference. If α and β are the angles of $\overrightarrow{p}_{\pi^+}$ and $\overrightarrow{p}_{\pi^-}$ relative to $\overrightarrow{p}$ respectively (see Figure 11), then, using the angle of the vertex, $\varphi = \alpha + \beta$. Using conservation of 3-momentum perpendicular to $\overrightarrow{p}$, one gets $|p_{\pi^+}|\,sin(\alpha) = |p_{\pi^-}|\,sin(\beta)$. By combining the two one gets $tan(\beta) = \frac{|p_{\pi^+}|sin(\varphi)}{|p_{\pi^+}|cos(\varphi)+|p_{\pi^-}|}$ and $\alpha = \varphi - \beta$, both of which can be calculated using the measured momenta from invariant mass calculation. p is then $p = |p_{\pi^+}|\,cos(\alpha) + |p_{\pi^-}|\,cos(\beta)$

References

[1] G.Bella , E.Etzion, Simulation of a High Energy Detector for Undergraduate Physics Students ,School of Physics and Astronomy, Raymond and Beverly Sackler Faculty of Exact Sciences, Tel Aviv University, 1994.

[2] A.Das, T.Ferbel, Introduction to Nuclear and Particle Physics, 2nd edition, World Scientific Publishing Co. Pte.Ltd, 2005.

[3] D.H.Perkins, Introduction to High Energy Physics, 4th edition, Cambridge University Press, 2000.

[4] P.A. Zyla et al. Particle Data Group, Prog. Theor. Exp. Phys. 2020, 083C01 (2020) and 2021 update <https://pdg.lbl.gov/>.

[5] CERN , Pulling together: Superconducting electromagnets. <https://home.cern/science/engineering/pulling-together-superconducting-electromagnets>, 2020.